Structural Design and Tensile Experiment of Connection Node between acrylic and Stainless Steel

Xiaohui Qian (qianxh@ihep.ac.cn)
Institute of High Energy Physics Chinese Academy of Sciences
Xiaoyan Ma
Institute of High Energy Physics Chinese Academy of Sciences
Yuekun Heng
Institute of High Energy Physics Chinese Academy of Sciences
Wei He
Institute of High Energy Physics Chinese Academy of Sciences
Zhonghua Qin
Institute of High Energy Physics Chinese Academy of Sciences
Jianxia Xiao
Jiangsu Domchampp New Material Technology Co. Ltd, Taixing Chian
Gaofeng Zhang
Jiangsu Domchamp New Material Technology Co. Ltd, Taixing China
Wei Cheng
Jiangsu Domchamp New Material Co. Ltd, Taixing, China
Lei Li
Jiangsu Domchamp New Material Technology Co. Ltd, Taixing, China
Shaojing Hou
Institute of High Energy Physics Chinese Academy of Sciences
Yatian Pei
Institute of High Energy Physics Chinese Academy of Sciences
Xiaoyu Yang
Institute of High Energy Physics Chinese Academy of Sciences
Zian Zhu
Institute of High Energy Physics Chinese Academy of Sciences

Original Article

Keywords: JUNO, acrylic connection node, Tensile experiment, Brittle material

Posted Date: January 18th, 2021

DOI: https://doi.org/10.21203/rs.3.rs-145371/v1

Abstract

Acrylic are widely used as load-bearing structural parts. In this study, the structural design, finite element analysis (FEA) and tensile experiment of the connection node of the acrylic spherical vessel designed for Jiangmen Underground Neutrino Observation (JUNO) are carried out. The acrylic connection node needs to withstand a tensile load of 90 kN for 20 years, and its ultimate bearing capacity is required to be 6 times the working load. Under working load, the stress of the acrylic structure should be less than 3.5 MPa. In the study, a connection node connecting acrylic and stainless steel is designed. By embedding the steel ring in the acrylic structure to connect with the support rod, the acrylic connection node can withstand high loads. A 1/4 symmetric model of connection node is established, and the FEA method is used to solve nonlinear problems such as material nonlinearity and frictional contact. The results of FEA show that the maximum principle stress of the connection node is about 2.92 MPa. By comparing the stress of the FEA results with the experimental results, the relative difference is 7.24 %, indicating that the FEA results are credible. The experiment results also show that the ultimate tensile load of the connection node can reach 1000 kN, which is about 11 times the working load. The breakdown of the connection node occurs at the sharp corner of the groove instead of the maximum stress point. Through the design, simulation and experiment of the connection node, for the brittle materials such as acrylic, the structure should avoid the defects such as sharp corner.

1. Introduction

Polymethyl methacrylate (PMMA) also known as acrylic, is widely used in basic scientific experiments [1-5]. One of the most important applications is that acrylic work as a load-bearing components. Then the bearing capacity and stress level of acrylic components become the most critical design indicators. According to a handbook of acrylics [6], the stress of the acrylic is required to be less than 5.5 MPa. For acrylic components that cannot be repaired in the long run, the stress requirements should be even more stringent. For example, the main structure of the detector of Sudbury Neutrino Observatory (SNO) [7] is an acrylic vessel with a diameter of 12 m and a thickness of 5 cm, which requires the stress of the acrylic to be less than 4.0 MPa [8]. In this study, a 35.4 m diameter acrylic vessel with a thickness of 12 cm in the Jiangmen Underground Neutrino Observation (JUNO) [9,10] is almost three times the diameter of the SNO acrylic vessel. This makes the support structures of the two acrylic vessels very different. Figure 1(a) shows the central detector of JUNO. The main structure is an acrylic spherical vessel supported by a stainless steel mesh shell. Figure 1(b) shows the acrylic spherical vessel. There are 590 acrylic connection nodes on the outer surface of the acrylic vessel. Figure 1(c) shows the details of the connection structure between the acrylic vessel and the stainless steel mesh shell. The support rod connects the acrylic connection node and the stainless steel mesh shell together. The density difference of the liquid inside and outside the acrylic vessel makes the acrylic vessel withstand more than 3,000 t of buoyancy. The buoyancy needs to be transmitted to the outer stainless steel mesh shell through the support rod. According to the finite element analysis (FEA) results of Li[11], the maximum tensile force of the support rod will reach 90 kN. Under this load, the stress of the acrylic structure should be controlled

below 3.5 MPa according to JUNO's requirements [10,12], and the ultimate bearing capacity of the connection node should be greater than 6 times the tensile load. It can be seen that the connection node becomes the most critical structure of the acrylic vessel.

At present, there are few designs of high-strength connection structures between acrylic and metal materials. Wang [13,14] designed a connection node with stainless steel plate embedded in an appended acrylic panel, shown in figure 2(a). The steel plate is a bearing structure that can avoid bending moments at the connection node. The appended panel is bonded on an acrylic spherical panel. The stress on the acrylic parts is about 10 MPa under the force of 140 kN and the ultimate bearing capacity of the node is about 300 kN. Hao [15] optimized the structure and manufacturing process of the node. Although the stress of the connection node does not decrease, the ultimate bearing capacity increases to 513 kN. For the node A, shown in figure 2(a), embedding a large stainless steel plate into the appended acrylic panel requires removing a large amount of acrylic material from the appended panel, thereby weakening the strength of the connection node. Another conceptual design of the connection node shown in figure 2(b) was designed by Lin [16]. It avoids the weakness of node A, but the higher appended acrylic panel will unavoidably create large bending moment at the bottom edge of appended panel.

In order to further improve the ultimate bearing capacity of the connection node and control the stress to be less than 3.5 MPa under the workload, this study designs a new connection node between the acrylic and the stainless steel. The FEA of the designed connection node is carried out to obtain the stress distribution at the node. Through the tensile test of the connection node, the ultimate bearing capacity of the connection node is well understood. Finally, the FEA results are validated with the experimental results.

2 Structure Design Of Connection Node And Experiment Device

2.1 Structure of connection node

Figure 3 shows the new structure of the acrylic connection node. The diameter of the appended acrylic panel is 900 mm and its thickness is 140 mm. There is an annular groove at the bottom of the appended panel. A stainless steel ring is assembled into the groove before the appended panel is bonded with an acrylic spherical panel. A gasket made of rubber is placed between the stainless steel ring and the acrylic. The top of the node is the bearing component, which will be connected to the steel ring by eight bolts. Through the bearing structure, the support rod and the connection node are hinged together to avoid bending moment on the connection node. The spherical panel size is designed to be 1800 mm×1800 mm for FEA modeling and prototype tests.

There are three main differences between the new connection node and the Type A node. Firstly, the appended panel cavity adopts a groove structure with the stainless steel ring embedded inside. The size of steel ring structure is small so that it can reduce the weakening effect on the appended panel structure. Secondly, the transition between the appended panel and the spherical panel adopts a large arc surface

to make a smooth transition in thickness to avoid sudden changes in stiffness. Finally, the acrylic structure and the stainless steel structure are separated by rubber gaskets to avoid hard contact between two parts.

2.2 Tensile test equipment

Figure 4 shows the equipment used to test the connection node prototype in tension. The connection node is put inside a square frame which is fixed on four piers at bottom. The connection node is connected with oil pump on the top of it, while the oil pump is fixed by a horizontal beam. The maximum force provided by the oil pump is 1000 kN. Space between the connection node and the square frame is filled with rubber and cement.

3 Finite Element Model

Figure 5 shows the material test curve of the acrylic. The red curve shown in figure 5(a) is the tensile test curve of the acrylic. When the material fractures, the material does not undergo plastic deformation. The maximum tensile stress is about 75 MPa. The tensile test result shows that the acrylic is a kind of brittle material. The black dotted curve is the compression test curve of the acrylic. As the stress increases, the material exhibits significant plastic deformation. The maximum compression stress of acrylic is about 113 MPa, which is higher than the tensile stress. The constitutive model of acrylic in low stress is linear as shown in figure 5(b). The mechanical properties of acrylic and stainless steel are shown in table 1.

Table 1 The mechanical properties of acrylic and stainless steel.

Item	Unit	acrylic	Stainless steel
Density:	kg/m3	1190	8000
Modulus of elasticity:	GPa	3	200
Poisson’s ratio:	—	0.35	0.3

The upper and lower gaskets are made of rubber. Figure 6 is the relationship between normal strain and normal stress of rubber. In the FEA model, Yeoh model is used to characterize the constitutive relationship of rubber.

Because the structure and load of the numerical model are symmetrical, a quarter of the connection node model is used in the abaqus finite element software, as is shown in Figure 7. There are two symmetry faces in the model. The boundary conditions between gasket and acrylic, bearing head and bearing seat are set to be frictional. The friction coefficient between gasket and acrylic is 0.5. The support piers at the bottom of the square frame are set to be fixed boundary. A tensile force of 90 kN is applied to the top of the bearing head. All parts of the model are divided by linear hexahedron meshes. Since the connection

node is mainly subjected to the bending stress, an 8-layer mesh is used in the thickness direction of the spherical panel to avoid an hourglass phenomenon caused by the using of reduced integrated element.

4 Fea Result

In this section, the FEA results of the connection node under the workload of 90 kN are shown. Figure 8 is the stress contour of the connection node. In the figure 8(a), the maximum Von Mises stress is 3.30 MPa, which occurs around the bolt hole**.** The Von Mises stress at the edge of the appended panel is 2.13 MPa. Figure 8(b) is the absolute maximum principal stress. The maximum principal stress is 2.92 MPa which also occurs around the bolt holes. The maximum principal stress at the edge of the appended panel is 2.57 MPa. The maximum compressive stress is 3.66 MPa in the annular groove where the lower gasket is in contact with the acrylic. The load is transferred from the steel ring and the lower gasket to the acrylic structure. The maximum compressive stress at the bottom face of the connection node is about 1.56 MPa. The top face of the connection node is mainly tensile stress.

When testing the ultimate bearing capacity of the node, it is believed that damage will occur at two locations first. One is located at the edge of the appended panel. This edge is where the bonding line is located, and it is also the second largest stress location. The reason for the large stress here is the inconsistent thickness of the node. The stresses of the node in the three directions of the cylindrical coordinate system at the edge of the appended panel are 2.44 MPa, 1.31 MPa, and 0.23 MPa, respectively, shown in figure 9. The stress in the R direction is the largest, so the node is prone to crack in the direction given in figure 9(a). When Wang[14] and Zhou[17] performed the node A experiments, Some nodes broke at the edge of the appended panel with a stepped structure. Therefore, the transition between the appended panel and the spherical panel should be smooth.

Another dangerous place is the corner of the annular groove, since acrylic is a brittle material and sensitive to sharp corners. The stress at the corners is not very large. However, the stress at the sharp corners increases as the mesh size decreases, and the stress shows a tendency of non-convergent. In the figure 9(a), the stresses at the four corners in the R direction are 1.23 MPa, 0.18 MPa, 0.62 MPa, and 0.37 MPa, respectively. The maximum stress occurs in the corner 1. The figure 10 shows the deformation of the groove on the symmetrical section. The angles of the corner 1 and 3 become larger under the tensile force. In prototype experiments, rounded corners are processed at the corner 1 and corner 4, as shown in figure 3. Limited by the manufacturing process, corner 2 and corner 3 are difficult to be rounded. Therefore, the connection node has a high risk of cracking at the corner 3 when a tensile force is loaded on it.

Figure 11 shows the displacement of the node. The maximum value of the total displacement is 2.15 mm, which is the same as the displacement in the Z direction.

5 Experimental Results

Several prototypes of connection nodes were tested. This study introduces the experimental process, displays the test results of a node, and analyzes the test results.

5.1 Instrumentation

The strain rosettes are used to monitor the stress of the node. Using cyanoacrylate glue (also called 502 glue) to bond the strain rosette to the acrylic surface will damage the acrylic surface and further affect the ultimate bearing capacity of the node. However, this negative effect can be reduced when the surface stress is compressive stress. Therefore, all strain rosettes are glued to the bottom surface of the node and distributed symmetrically, as shown in Figure 12. The 45 degree strain rosette shown in figure 13 contains three strain gauges at a certain angle which can calculate the principle stress on the surface of the connection node. The principle stress can be expressed as:

$$\sigma_{1,2} = \frac{E}{1-\mu^2}\left[\frac{1+\mu}{2}(\varepsilon_0+\varepsilon_{90}) \pm \frac{1+\mu}{\sqrt{2}}\sqrt{(\varepsilon_0-\varepsilon_{45})^2+(\varepsilon_{45}-\varepsilon_{90})^2}\right], \quad (1)$$

$$\sigma_3=0, \quad (2)$$

Then the Von Mises stress can be calculated from the principal stress.

$$\sigma_{VM} = \sqrt{(\sigma_1-\sigma_2)^2+(\sigma_2-\sigma_3)^2+(\sigma_3-\sigma_1)^2}, \quad (3)$$

5.2 Tensile test results

Figure 14 is the tensile test curves. The time-force curve shown in Figure 14(a) includes three stages, namely loading, holding and unloading. The loading rate is about 30 kN/min. When the force reaches 1000 kN which is the maximum force that oil pump can provide, the force will remain in about ten minutes. The unloading rate is about 50 kN/min. The total time of each test is about 70 minutes.

Figure 14(b) is the displacement-force curve. After unloading the force, the displacement-load curve is not a closed loop. This is mainly due to the plastic deformation of the components and the local fracture of the acrylic.

- Time-force curve
- Displacement-force curve

After the experiment, cracks were found at the corner 3 of the annular groove, as is shown in the figure 15. The locations of the crack are consistent with the previous description in section 4. Corner 3 is difficult to machine into a round corner, and there is tensile stress. The video shows that the connection node began to crack during the second stage. Therefore, the ultimate bearing capacity of this node is about 1000 kN.

5.3 Comparison of experimental results and FEA results

Table 2 is the stress comparison of experiment and FEA results. There are 20 strain rosettes in total at the bottom face of the connection node that are divided into 7 zones. The maximum coefficient of variation is 32.37 % happened at zone VII. Due to a small amount of test data and small test values, the test results in this area vary greatly. Except for this zone, the maximum value of the coefficient of variation is 6.43%, indicating that the measurement data is reliable. The maximum absolute relative difference between experimental results and FEA results is 7.24 % at zone III, indicating that the FEA results are consistent with the experimental results.

Table 2 Stress comparison of experiment and FEA results

Zone	Measurement point	Stress [MPa]	Average Stress [MPa]	coefficient of variation [%]	FEA results [MPa]	Relative difference [%]
I	A1	1.47	1.54	6.43	1.54	0
	A2	1.61				
II	B11	1.48	1.45	5.88	1.52	4.83
	B12	1.37				
	B13	1.56				
	B14	1.40				
III	B21	1.45	1.42	2.99	1.52	7.04
	B22	1.39				
IV	C11	1.45	1.52	3.86	1.63	7.24
	C12	1.50				
	C13	1.59				
	C14	1.53				
V	C21	1.57	1.62	4.79	1.74	7.21
	C22	1.68				
VI	D11	0.84	0.78	5.54	0.75	-3.85
	D12	0.76				
	D13	0.78				
	D14	0.74				
VII	D21	0.64	0.83	32.37	0.77	-7.23
	D22	1.021				

6 Conclusions

In this study, a high-strength connection node structure is designed to connect the acrylic and stainless steel. The structure of this node is different from the previous design by Wang [13]. By reducing the size of embedded stainless steel parts, smoothing the transition between the appended acrylic and the spherical acrylic panel, and separating the acrylic and stainless steel with rubber, the ultimate bearing capacity of the connection node is improved and the stress under the workload of 9 kN is controlled to be less than 3.5 MPa. Through the FEA and tensile experiment of the connection node, the following conclusions can be obtained:

(1) The acrylic is a kind of brittle material. The fracture of acrylic parts usually occurs at some defects such as sharp corners. Therefore, for the structural design of brittle materials, such defects should be avoided.

(2) According to the FEA results, the maximum principle stress of the connection node under the force of 90 kN is 2.92 MPa, which meets the requirement of less than 3.5 MPa.

(3) According to the experimental results, the ultimate bearing capacity of the connection node can reach about 1000 kN, which is more than 11 times of the workload.

(4) In the comparison between FEA and experimental results, the maximum relative different of stress is 7.24 %. This shows that the FEA results are in good agreement with the experimental results.

7 Declaration

Availability of data and materials

The datasets supporting the conclusions of this article are included within the article.

Competing interests

The authors declare that they have no competing interests.

Funding

This work has been supported by the Strategic Priority Research Program of the Chinese Academy of Sciences (Grant No. XDA10010200), the Youth Innovation Promotion Association of the Chinese Academy of Sciences (Grant No. 292020000087).

Authors' contributions

Not applicable.

Acknowledgements

The authors would like to express their gratefulness to Tao Chen and Chang Liu from China Academy of Building Research.

References

1. Cao J., Luk, K.B., An overview of the daya bay reactor neutrino experiment, Nuclear Physics B 908, 62-73 (2016).
2. Amaudruz P.A., Baldwin M., Batygov M., et al, Design and construction of the DEAP-3600 dark matter detector. Astroparticle Physics, 1-23 (2019).
3. Morgante E, Racco D, Rameez M, et al. The 750 GeV Diphoton excess, Dark Matter and Constraints from the IceCube experiment, Journal of High Energy Physics, 7, 141-164 (2016).
4. Hashim H., Adam N. I., Zaki N.H.M., Mahmud Z.S., Said C.M.S., Yahya M.Z.A., Ali A.M.M, Natural rubber-grafted with 30% Poly (methylmethacrylate) characterization for application in lithium polymer battery, Conference on Science and Social Research 2010 (CSSR 2010), Kuala Lumpur, Malaysia, 485-488 (2010).
5. Mishra S., Sen G., Microwave initiated synthesis of polymethylmethacrylate grafted guar (GG-g-PMMA), characterizations and applications, International Journal of Biological Macromolecules, 48(4), 688-694 (2011).
6. Strachiw J. D., Handbook of acrylics for submersibles hyperbaric chambers and aquaria, 833-856, Best publishing company (2003)
7. Hallin A.L., The Sudbury Neutrino Observatory, Nuclear Physics, 908, 30-51 (2000).
8. Ewan G.T., The Sudbury Neutrino Observatory, Nuclear Instruments and Methods in Physics Research Section A-accelerators Spectrometers Detectors and Associated Equipment, 1, 172-207 (2000)
9. An F.P., An G.P., An Q., Antonelli V., et al., Neutrino Physics with JUNO, Journal of Physics G, 43, 030401 (2016)
10. Qian X.H., Ma X.Y., Qin Z.H., et al. Analysis of glass shell's thermal stress based on orthogonal experiment[J]. Journal of Mechanical Engineering ,2019, 55(12): 91-98.
11. Li H.F., Zhu Z.Y., Shu W.N, Qin K, Heng Y.K., Wang Z., Wang Y., Zheng Y.F., Design and research of the main stainless steel structure of the central detector of Jiangmen Underground Neutrino Observatory, Building Structure, 48, 92-97 (2018)
12. Qian X.H., Ma X.Y., Heng Y.K, et al. Structure design and compression experiment of the supporting node for JUNO PMMA detector[J]. Radiat Detect Technol Methods, 2020, 4: 345–355.
13. Wang Y.Q., Zong L., Heng Y.K., Wang, Z.Y., Zhou Y., Hou S.J, Qin Z.H., Ma X.Y., Application of an acrylic vessel supported by a stainless-steel truss for the JUNO central detector, Science China Technological Sciences, 57, 2523-2529 (2014)
14. Wang Z.Y. Wang Y.Q. Du X.X. Heng Y.K., Study on the Fracture Properties of the PMMA Structure for the JUNO Central Detector, Ksce Journal of Civil Engineering, 6, 2584-2597 (2019)
15. Hao J.J., Qian X.H., Ma X.Y., Heng Y.K., Wang L.S., Wang Y.Q., Design and test of connecting point between acrylic sphere and stainless steel truss for JUNO central detector, Journal of Mechanical Strength, 5, 1123-1129, (2016)
16. Lin Y.C., Design and FEA simulation of central detector and support node for JUNO experiment, 39-60, National Taiwan University (2017)

17. Zhou Y., Structural style selection and connections bearing behavior reserach for JUNO central detector, 92-108, Chongqing University (2014)

Biographical Notes

Xiaohui Qian, born in 1987, is PhD from *University ofChinese Academy of Science, Beijing, China* and an engineer at *Institute of High Energy Physics, China*. He received his bachelor degree from *Chinese Academy of Science, China*, in 2010. His research interests include Multiphysics Coupling Simulation, PMMA properties research and neutrino detector design.

Tel: +86-010-88236083; E-mail:qianxh@ihep.ac.cn

Xiaoyan Ma, is currently a senior engineer at *Institute of High Energy Physics, Chinese Academy of Science, Beijing, China*.

Tel: +86-010-88236083; E-mail:maxy@ihep.ac.cn

Yuekun Heng, is currently a reseacher at *Institute of High Energy Physics, Chinese Academy of Science, Beijing, China*.

E-mail:hengyk@ihep.ac.cn

Wei He, is currently a senior engineer at *Institute of High Energy Physics, Chinese Academy of Science, Beijing, China*.

E-mail:hewei99@ihep.ac.cn

Zhonghua Qin, is currently an associate researcher at *Institute of High Energy Physics, Chinese Academy of Science, Beijing, China*.

E-mail:hewei99@ihep.ac.cn

Jianxia Xiao, is currently a Deputy General Manager at Jiangsu Domchamp New Material Technology Co., Ltd.*, Taixing, China*.

E-mail: xiaojianxia78@163.com

Gaofeng Zhang, is currently an engineer at Jiangsu Domchamp New Material Technology Co., Ltd.*, Taixing, China*.

E-mail: 3228705198@qq.com

Wei Cheng, is currently an engineer at Jiangsu Domchamp New Material Technology Co., Ltd.*, Taixing, China*.

E-mail: 511389266@qq.com

Lei Li, is currently an engineer at Jiangsu Domchamp New Material Technology Co., Ltd., *Taixing, China*.

E-mail: 27187899@qq.com

Shaojing Hou, is currently an engineer at *Institute of High Energy Physics, Chinese Academy of Science, Beijing, China*.

E-mail: housj@ihep.ac.cn

Yatian Pei, is currently an engineer at *Institute of High Energy Physics, Chinese Academy of Science, Beijing, China*.

E-mail: peiyt@ihep.ac.cn

Xiaoyu Yang, is currently an engineer at *Institute of High Energy Physics, Chinese Academy of Science, Beijing, China*.

E-mail: yangxy@ihep.ac.cn

Zian Zhu, is currently a reseacher at *Institute of High Energy Physics, Chinese Academy of Science, Beijing, China*.

E-mail: zhuza@ihep.ac.cn

Figures

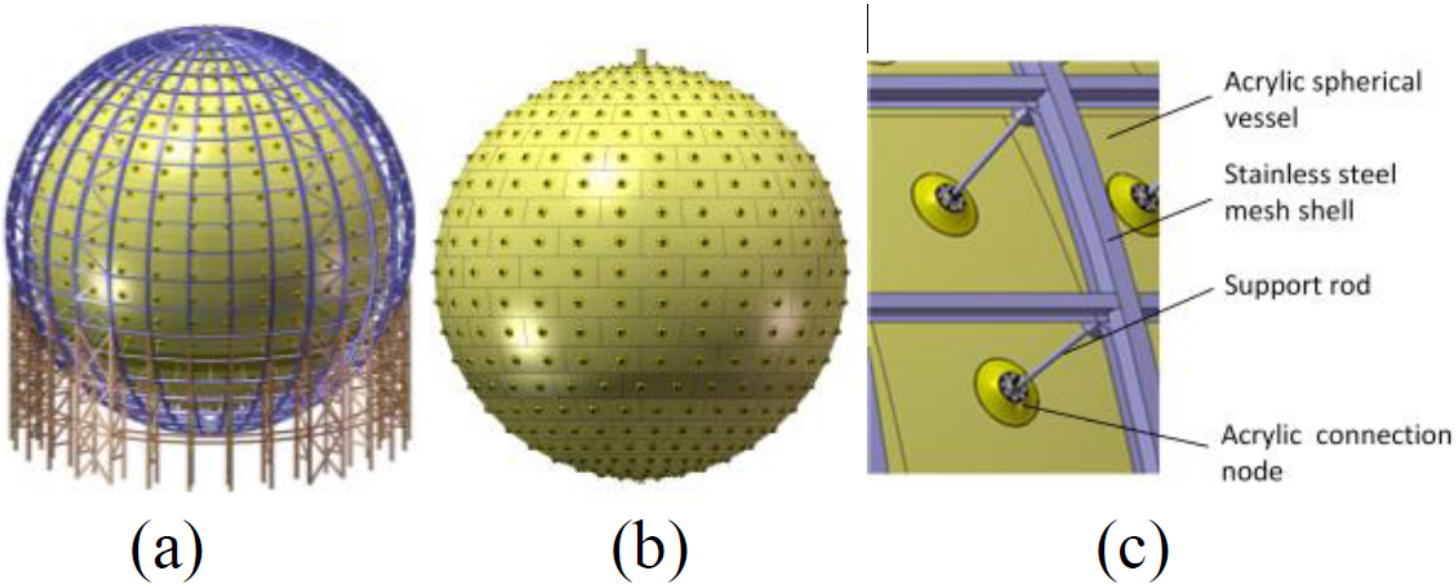

Figure 1

tral detector of JUNO. (a) Acrylic spherical vessel supported by stainless steel mesh shell. (b) Acrylic spherical vessel. (c) Connection structure between acrylic vessel and stainless steel mesh shell.

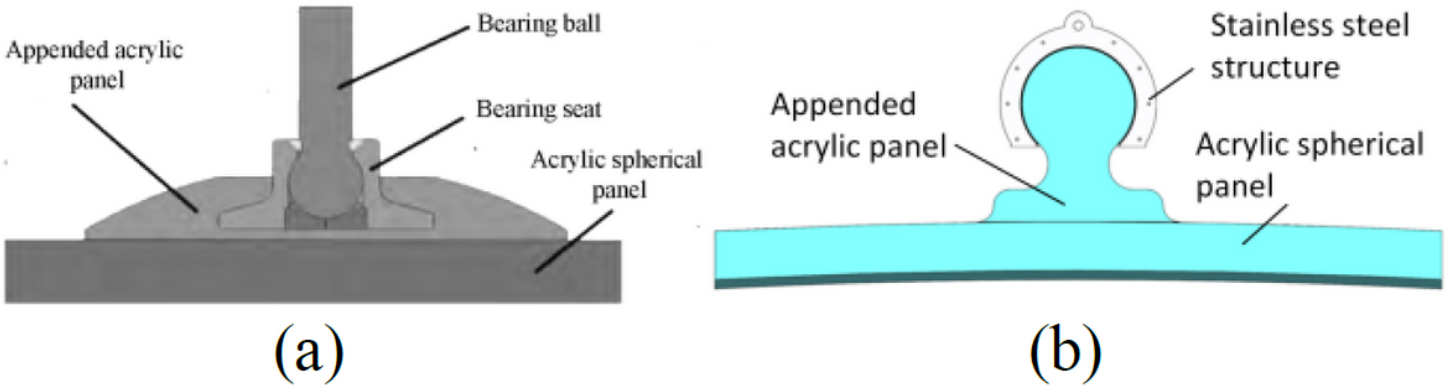

Figure 2

Structure of acrylic connection node. (a) Type-A node or Node A. (b) Type-B node or Node B.

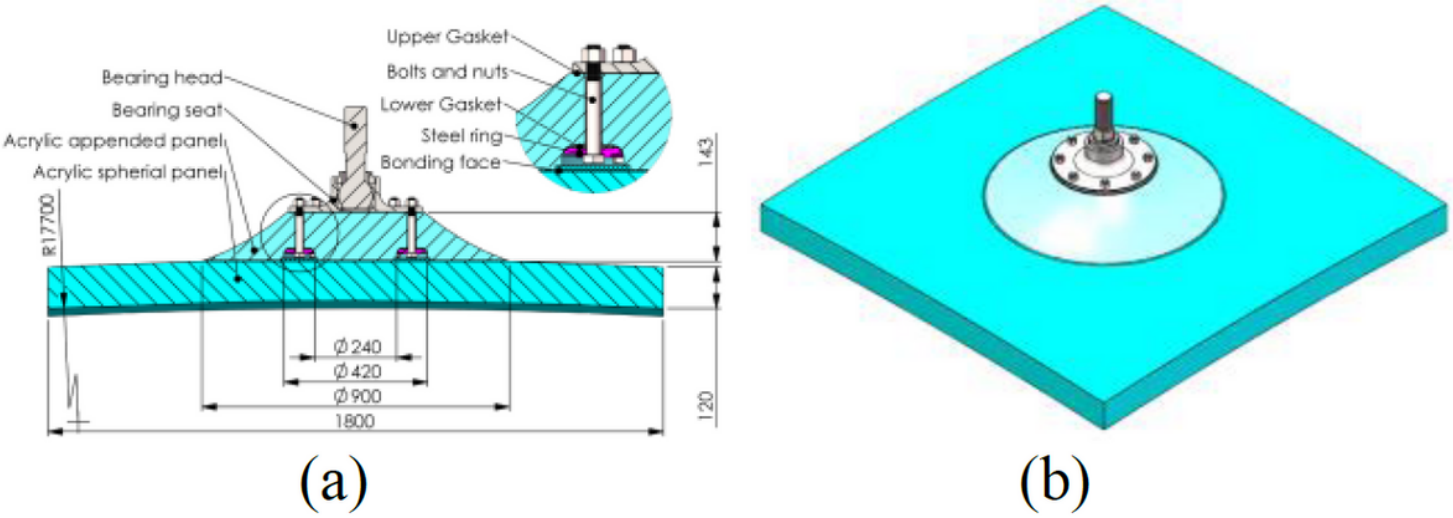

Figure 3

New structure of acrylic connection node. (a) Cross-section of connection node. (b) Axis view.

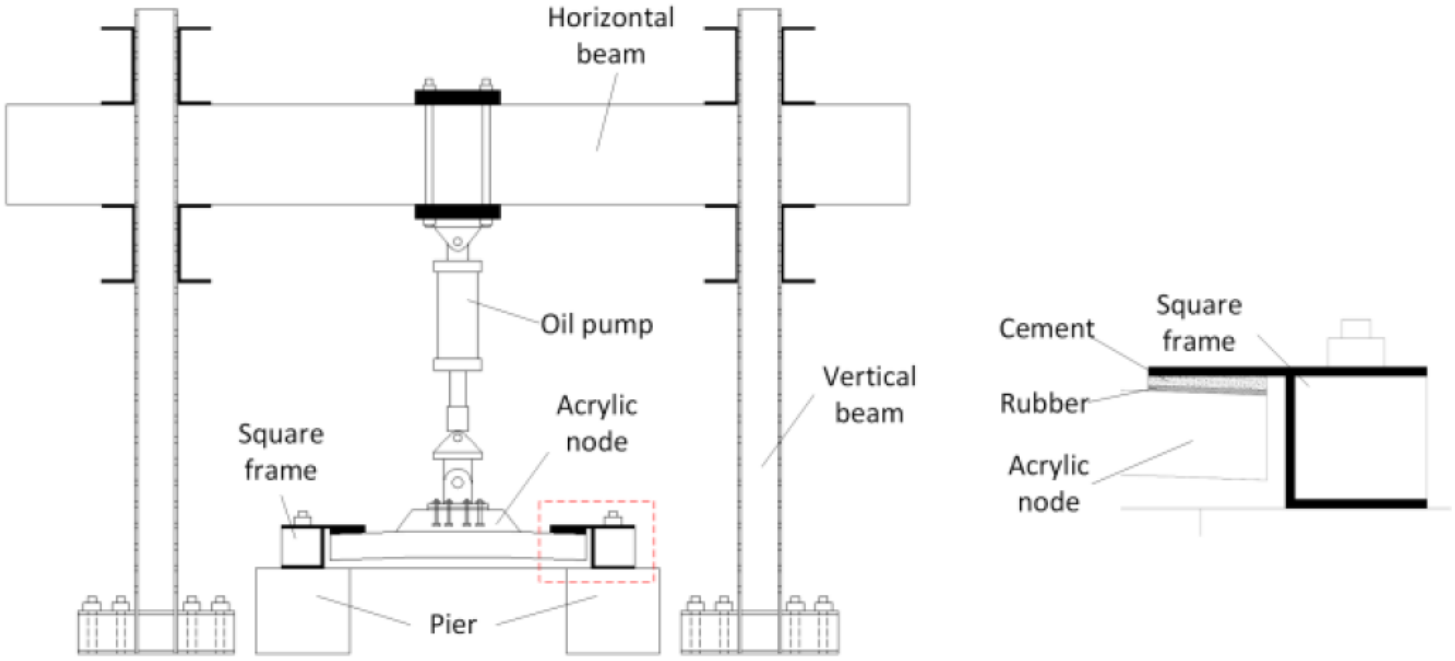

Figure 4

Tensile test equipment for connection nodes

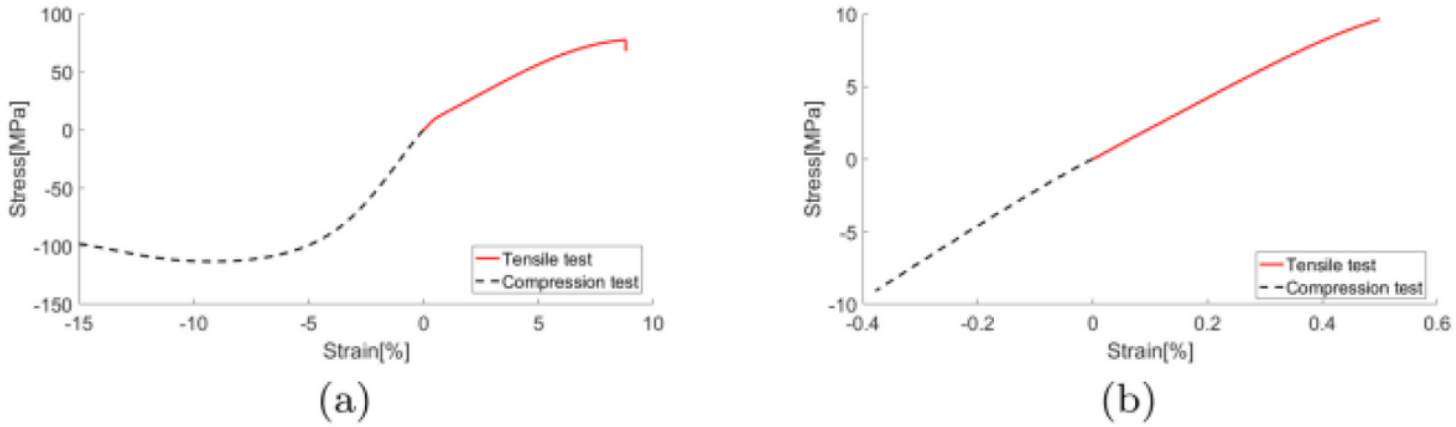

Figure 5

Material test of acrylic. (a) Tensile and compression test. (b) Test curve in low stress.

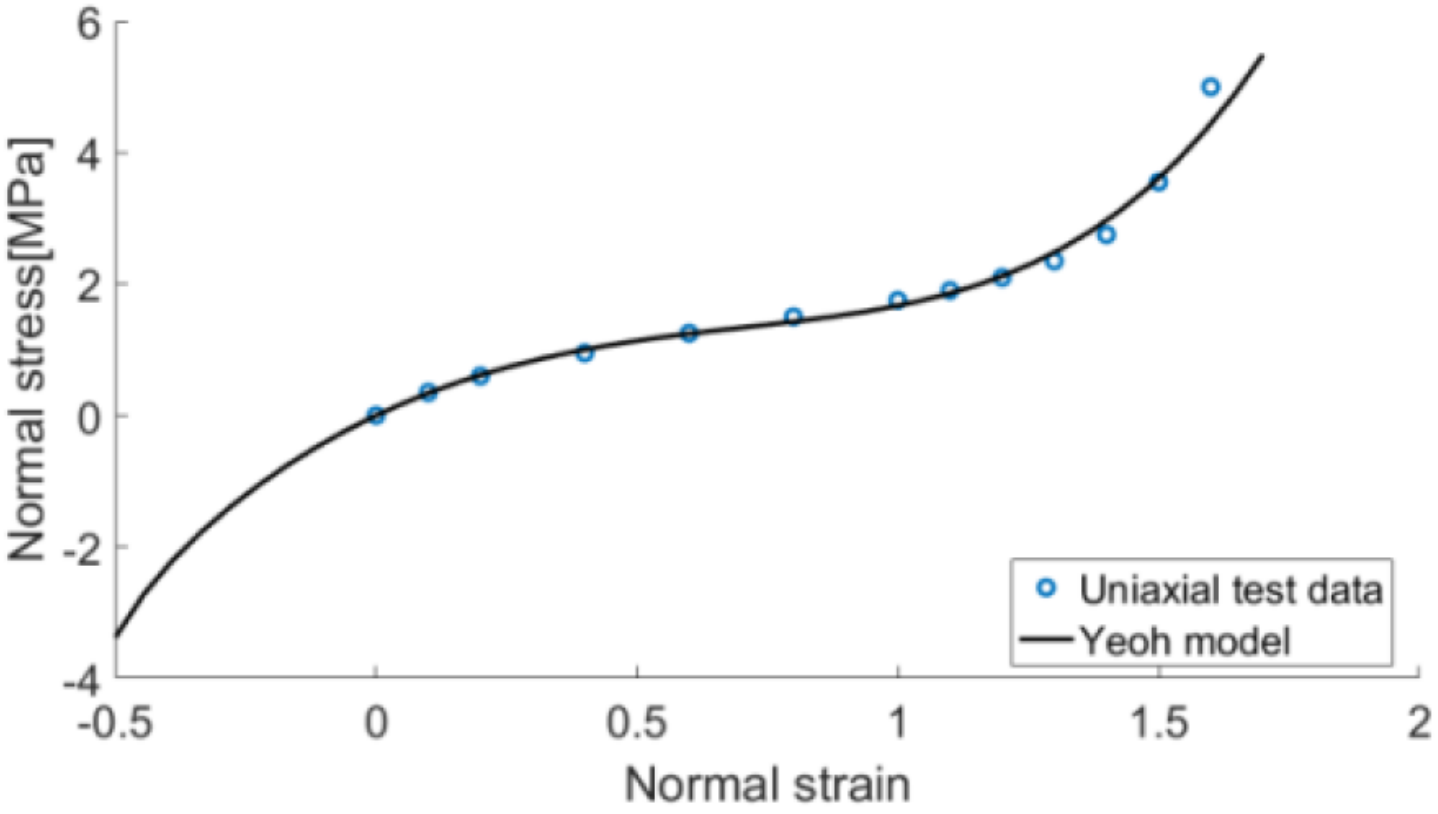

Figure 6

Yeoh model of rubber matched with uniaxial test data.

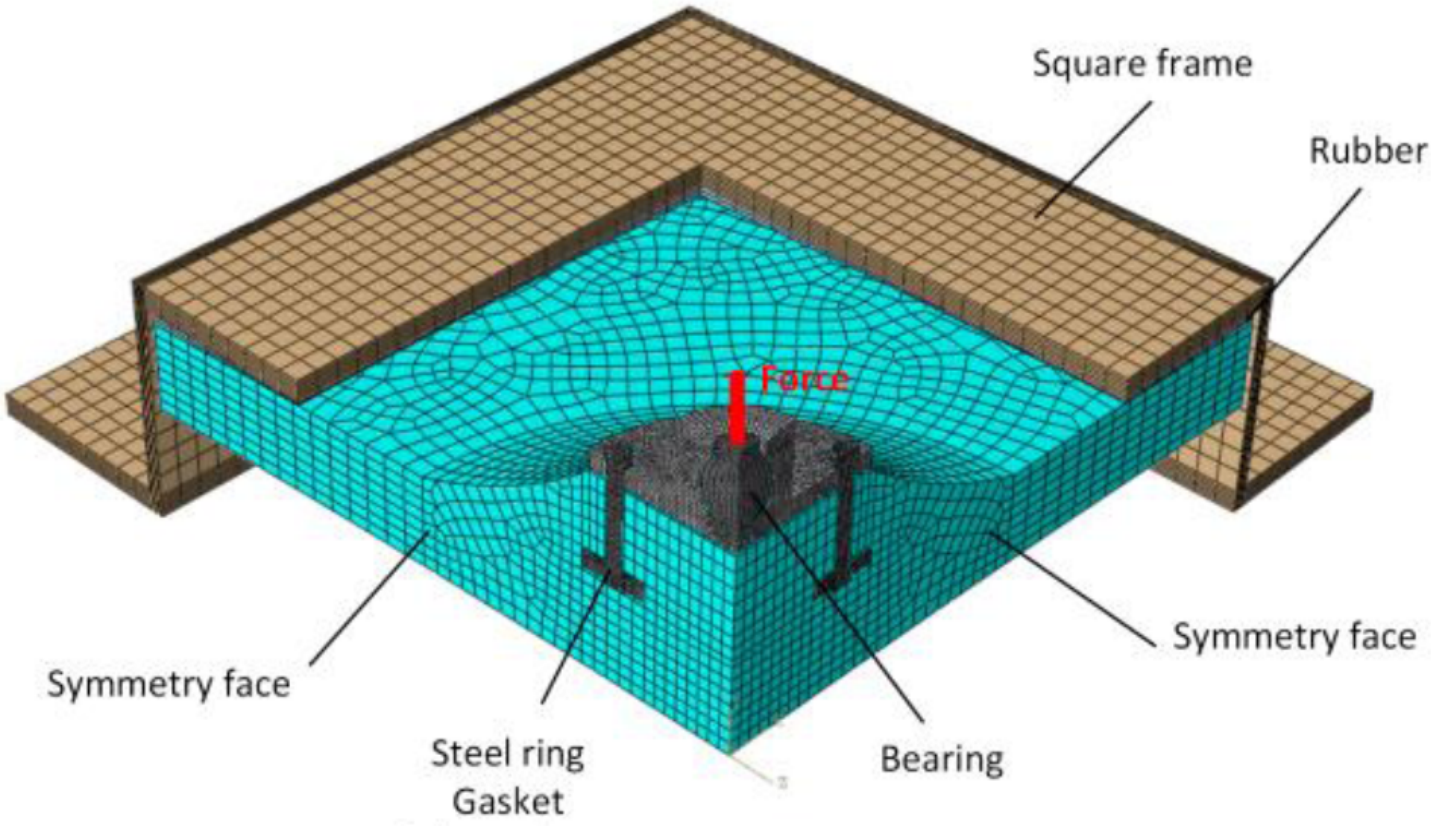

Figure 7

A quarter model of connection node in FEA.

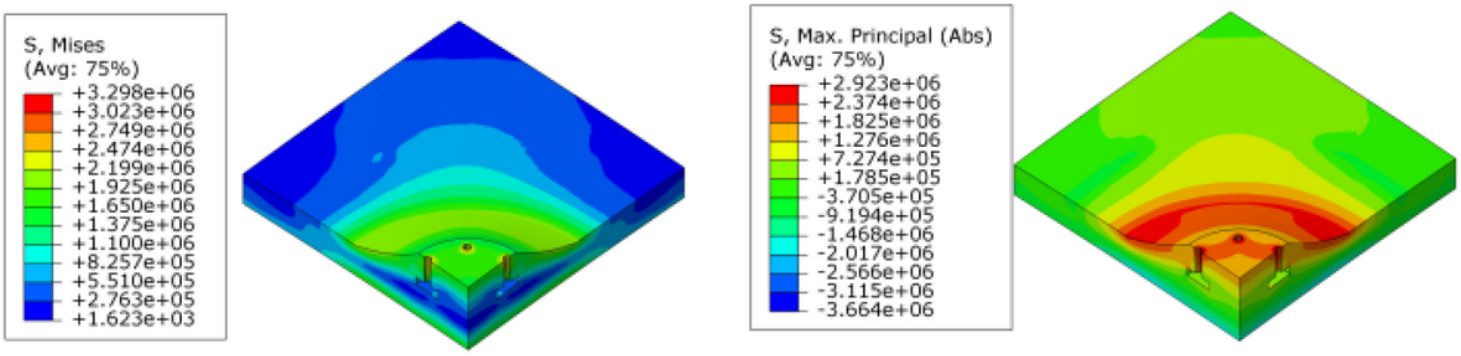

Figure 8

The stress of connection node under 90 kN force; (a) Von Mises stress; (b) Absolute maximum principal stress.

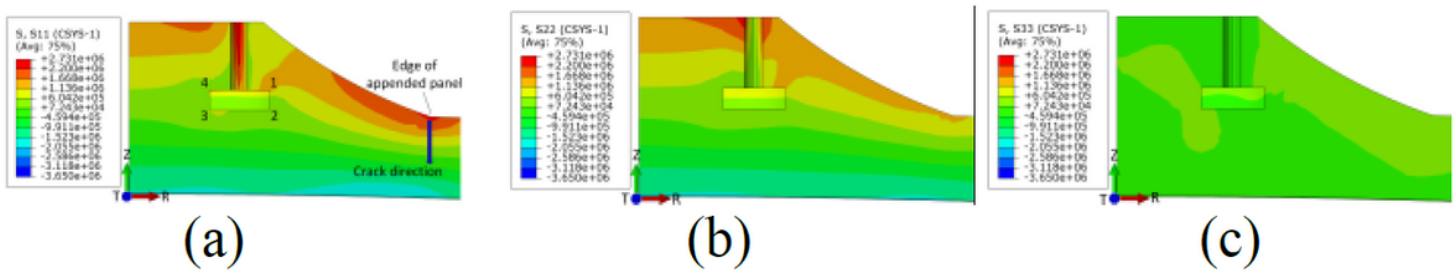

Figure 9

The stress of symmetry face in cylindrical coordinates; (a) R direction; (b) T direction; (c) Z direction.

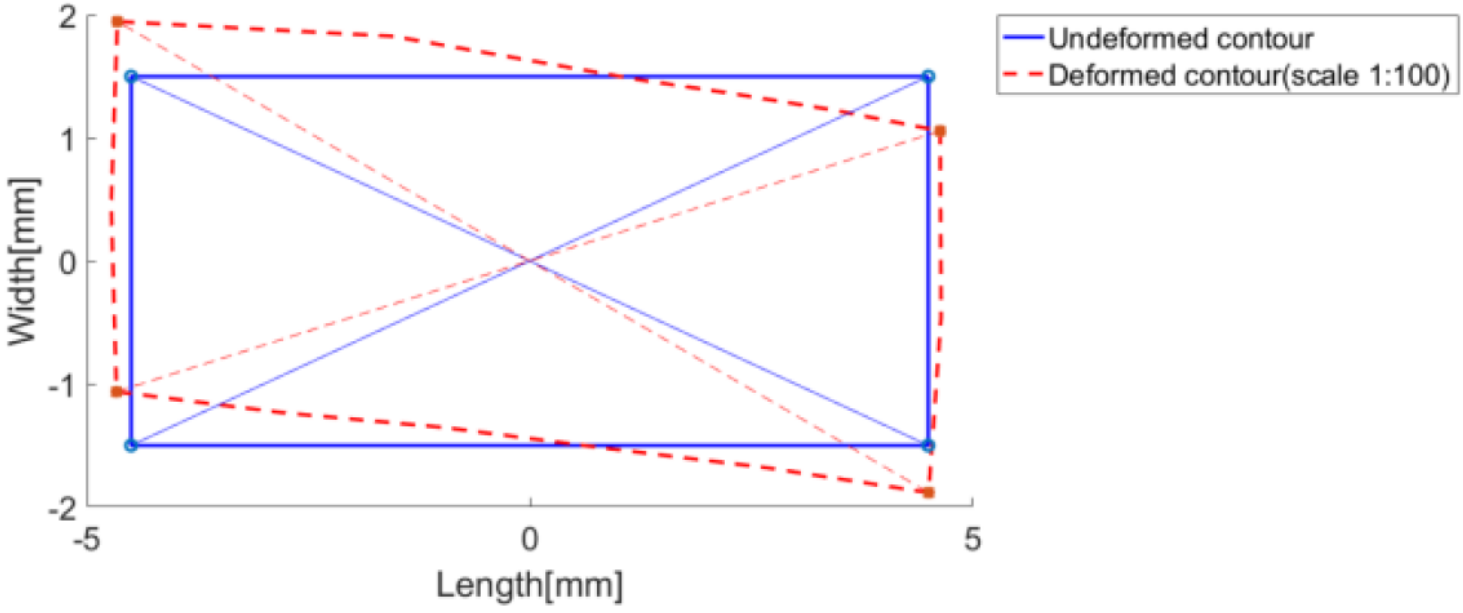

Figure 10

The deformation of the groove on the symmetrical section.

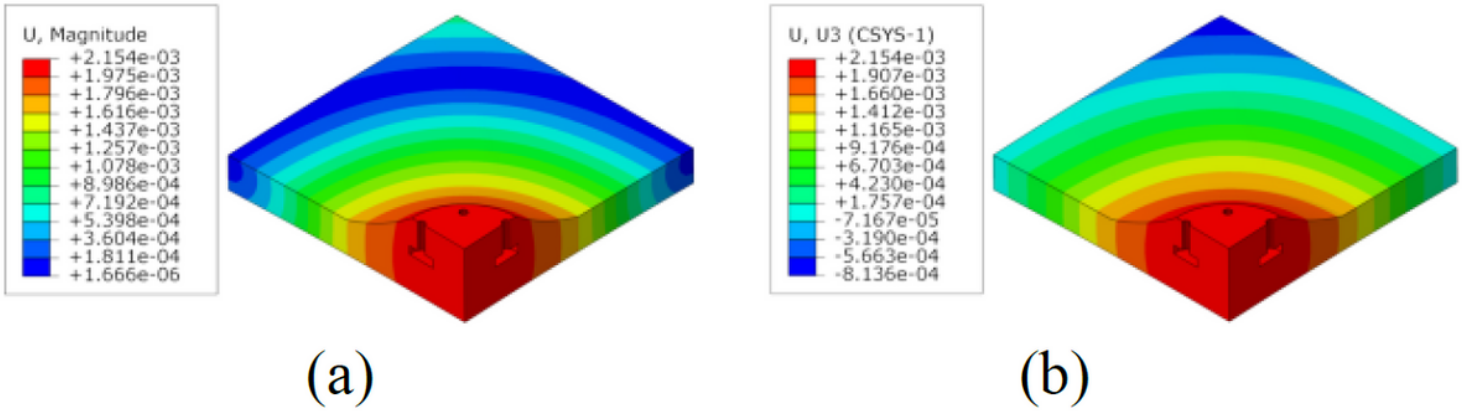

Figure 11

Displacement of connection node; (a) Total displacement; (b) Z-direction.

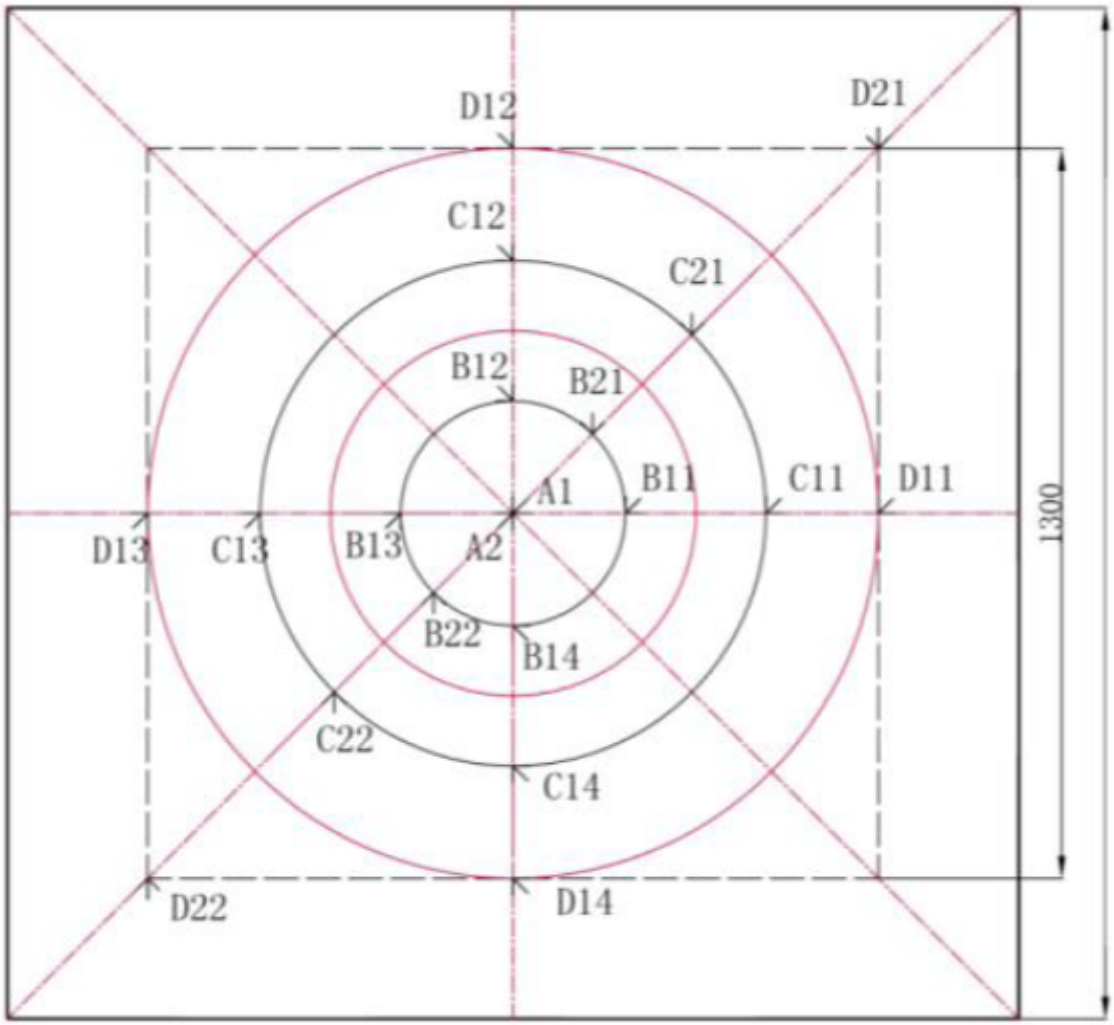

Figure 12

Location of strain rosettes.

Figure 13

45 degree strain rosette.

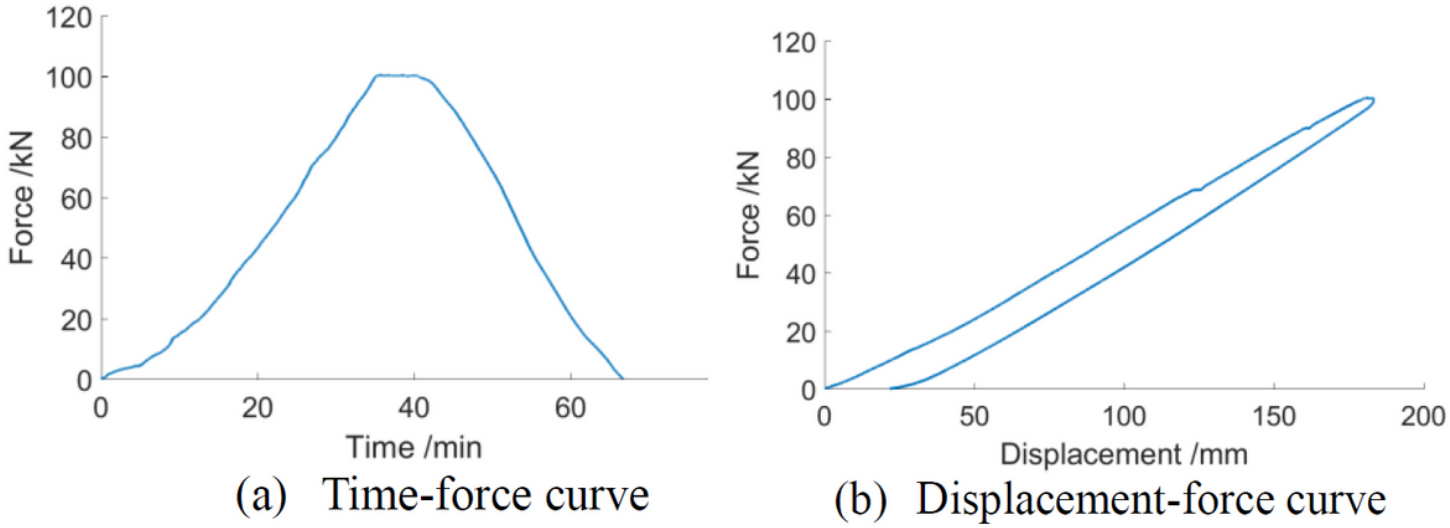

Figure 14

Tensile test curves.

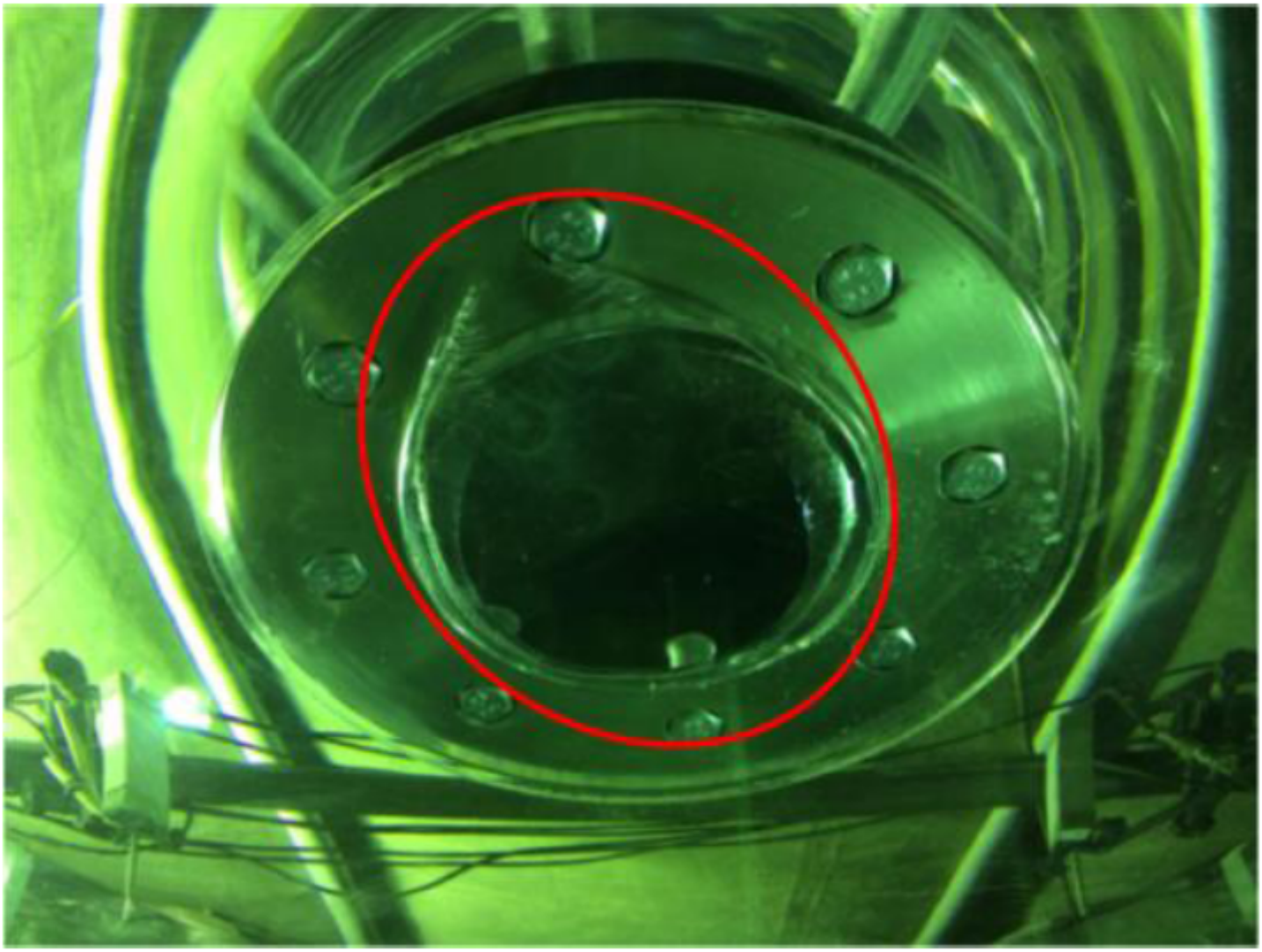

Figure 15

A picture to show cracks at corner 3 of annular groove.